New Analytical Methods

Generic haptens synthesis, broad-specificity monoclonal antibodies preparation and ultrasensitive ELISA for five antibacterial synergists in chicken and milk

Hongfang Li, Shaoqin Ma, Xiya Zhang, Chenglong Li, Baolei Dong, Mari Ghulam Mujtaba, Yujie Wei, Xiao Liang, Xuezhi Yu, Kai Wen, Wenbo Yu, Jianzhong Shen, and Zhanhui Wang

J. Agric. Food Chem., **Just Accepted Manuscript** • DOI: 10.1021/acs.jafc.8b03834 • Publication Date (Web): 25 Sep 2018

Generic hapten synthesis, broad-specificity monoclonal antibodies preparation and ultrasensitive ELISA for five antibacterial synergists in chicken and milk

Hongfang Li [a], Shaoqin Ma [a], Xiya Zhang [b], Chenglong Li [a], Baolei Dong [a], Mari Ghulam Mujtaba [a], Yujie Wei [a], Xiao Liang [c], Xuezhi Yu [a], Kai Wen [a], Wenbo Yu [a], Jianzhong Shen [a], Zhanhui Wang [a,*]

[a] *Beijing Advanced Innovation Center for Food Nutrition and Human Health, College of Veterinary Medicine, China Agricultural University, Beijing Key Laboratory of Detection Technology for Animal-Derived Food Safety Beijing Laboratory for Food Quality and Safety, 100193 Beijing, People's Republic of China*

[b] *College of Food Science and Technology, Henan Agricultural University, 450002 Zhengzhou, People's Republic of China*

[c] *College of Veterinary Medicine, Qingdao Agricultural University, 266109 Qingdao, People's Republic of China*

* *Author to whom correspondence should be addressed*

Tel: +86-10-6273 4565

Fax: +86-10-6273 1032

E-mail: wangzhanhui@cau.edu.cn

ABSTRACT： An antibody with broad-specificity and principally depending on hapten structure and size is a key reagent for developing a class-selective immunoassay. In the present study, three new generic haptens of antibacterial synergists (ASGs) were proposed using trimethoprim as the start molecule. These haptens contained carboxyl groups on the *meta* position of trimethoxybenzene for conjugating to protein, while, the common moiety of ASGs, i.e., diaminopyrimidine, was intentionally and maximally exposed to the immune system in animals in order to induce antibodies with broad-specificity against ASGs. Five monoclonal antibodies (mAbs) were finally obtained, and 5C4 from the hapten with a short spacer arm, named Hapten A, showed not only uniform broad specificity but also high affinity to all five ASGs. We further determined the possible recognition mechanism of mAbs in terms of conformational and electronic aspects. An indirect competitive ELISA (icELISA) based-5C4 was established and exhibited IC_{50} values of 0.067–0.139 μg L^{-1} with cross-reactivity (CR) of 48.2%–418.7% for the five ASGs in buffer under optimal conditions. The calculated limits of detection of the icELISA for chicken and milk were 0.06 μg kg^{-1}–0.8 μg kg^{-1} and 0.05 μg L^{-1}–0.6 μg L^{-1}, respectively. The recoveries in spiked chicken and milk samples were 75.2%–101.4% with a coefficient of variation less than 14.3%. In conclusion, we developed, for the first time, a rapid and reliable icELISA for ASGs with significantly improved sensitivity and class-selectivity.

41 **KEY WORDS:** antibacterial synergists, generic haptens, broad specificity antibodies,

42 high sensitivity, food samples

■ INTRODUCTION

Antibacterial synergists (ASGs, shown in Figure 1a), also known as sulfonamide potentiators, are a group of dihydrofolate-reductase inhibitors that function by blocking folic acid metabolism in bacteria.[1] ASGs are commonly used in combination with sulfonamides or other antimicrobials, such as fluoroquinolones, β-lactams and aminoglycosides, and are efficient in inhibiting Gram-positive and Gram-negative bacteria.[2-4] To date, the ASG family consists of 9 drugs, including trimethoprim (TMP), diaveridine (DVD), brodimoprim (BOP), ormetoprim (OMP), baquiloprim (BQP), tetroxoprim (TXP), metioprim (MTP), aditoprim (ADP) and iclaprim (ICL). Of these ASGs, ADP and DVD are exclusively used in animals, while, ICL is used in humans and the remainder are both human and veterinary medicines.[1,5-8] DVD, OMP, and especially TMP are the most commonly used medicines in animal husbandry for the treatment of bacterial and protozoal diseases.[9] For example, compounds of TMP/sulfadiazine are used for urinary, gastrointestinal and respiratory tract infections and compounds of DVD/sulfaquinoxaline are used for antiprotozoal drugs in food animals.[4]

However, the irrational and excessive use of ASGs could result in residues in the food chain. The residues of ASGs create a potential threat to human health and ecosystem, including chromosome variations, thrombocytopenia, leukopenia, emesis, nausea and antibiotic-resistance.[10] Therefore, the maximum residue limits (MRLs) of ASGs in some food matrices have been established. The MRLs for TMP have been

set at 50 μg kg^{-1} in edible tissues including muscle, liver, kidney, fat and milk in most countries and the MRL for DVD in chicken is 50 μg kg^{-1} in Japan. The MRL of BQP has been set at 30 μg kg^{-1} (in milk) and 50 μg kg^{-1} (in porcine liver) by European Union.[11-14] Thus, a sensitive and reliable method is essential to be established to detect residues of ASGs in animal-derived foods. Instrumental methods are currently the most commonly reported techniques for the quantification of ASGs, and include gas chromatography and mass spectrometry,[15] high performance liquid chromatography–tandem mass spectrometry[1,16] and high-performance liquid chromatography.[17] Most of these instrumental methods are used for the simultaneous detection of TMP and sulfonamides rather than ASGs alone. Although instrumental methods are accurate and sensitive, complex extraction steps are always necessary, which are not appropriate for screening numerous test samples in a short term. As an effective alternative, immunoassay methods, just like enzyme-linked immunosorbent assay (ELISA), possess the merit of simplicity and cost-effectiveness, which make it particularly convenient to achieve screening purposes. Nowadays, simultaneous detection of several analytes using immunoassay has attracted increasing attention. Kuang's research group worked on the development of multi-analyte immunoassays, i.e., the simultaneous detection of 26 sulfonamide, 32 (fluoro) quinolones and so on.[18-21]

At present, a few immunoassays have been developed to analyze TMP residues only.[22-27] For effective surveillance, an icELISA which can detect multiple ASGs at

the same time would be preferable. To realize this goal, the preparation of antibodies with broad-specificity for ASGs is essential. To author's knowledge, there exist no reports on the production of antibodies with broad-specificity or the development of a class-selective ELISA. Hapten design is a critical procedure for generating antibodies with the desired affinity and specificity. As shown in Table 1, two haptens were synthesized to produce antibodies against TMP and showed negligible cross-reactivity (CR) with other ASGs. In the present study, we prepared three generic haptens of ASG with different spacer arms and broad-specificity mAbs against ASGs were obtained. An ultra-high sensitive indirect complete (icELISA) based on the broad-specificity mAbs was developed for the simultaneous detection of five ASGs (TMP, DVD, OMP, BOP and BQP) in chicken and milk samples. The performance of the icELISA was assessed using fortified and recovery studies.

■ MATERIALS AND METHODS

Materials. TMP, DVD and OMP were bought from Dr. Ehrenstorfer Gmbh (Ausburg, Germany). BOP and 3, 4, 5-trimethoxycinnamic acid, 5-(3, 4, 5-trimethoxybenzoyl)-2, 4-pyrimidinediamine (TBP), 3, 4, 5-trimethoxyphenylacetic acid, and gallic acid trimethyl ether were obtained from J & K Chemical Technology (Beijing, China). BQP, 2, 4-diaminopyrimidine, 2, 4-diamino-6-(4-fluorophenyl) pyrimidine, 5-phenyl-4-pyrimidinamine, pyrimethamine, 3-(3, 4, 5-trimethoxyphenyl) propionic acid, sulfaguanidine, sulfamethizole, sulfamerazine, norfloxacin and

furazolidone were supplied by Sigma–Aldrich (St. Louis, MO, USA). Hemocyanin from *megathura crenulata* (KLH), ovalbumin (OVA), bovine serum albumin (BSA), hypoxanthine aminopterin thymidine (HAT), complete and incomplete Freund's adjuvant, poly (ethylene glycol) (PEG) 1500, fetal calf serum were acquired from Sigma–Aldrich (St. Louis, MO, USA). Goat anti-mouse IgG (HRP labeled) and mouse mAb isotyping kit were obtained from Bio-Rad Laboratories, Inc. (Hercules, CA, USA). Cell culture medium (DMEM) was supplied by Thermo Fisher Scientific Inc. (Waltham, MA, USA). TMB substrate, N, N-dicyclohexylcarbodiimide (DCC) and N-hydroxy succinimide (NHS) and were purchased from Beyotime (Shanghai, China). The remaining chemical reagents were supplied by Sinopharm Chemical Reagent, Inc. (Beijing, China). Flat-bottomed high-binding polystyrene ELISA plates were obtained from Corning Life Sciences (New York, NY, USA). The buffer solutions used are listed in *Supporting Information*.

Instruments. The chemical structures of the haptens were confirmed by liquid chromatography triple quadrupole mass spectrometry (Agilent Technologies, Santa Clara, USA) and nuclear magnetic resonance spectrometry (NMR) DRX-600 (Bruker, Rheinstetten, Germany). The conjugation ratio was determined by matrix-assisted laser desorption ionization time of flight mass spectrometry (MALDI–TOF-MS) (Bruker, Rheinstetten, Germany). Values of optical density (OD) were measured using Multiskan FC microplate reader (Thermo Scientific).

Synthesis of Haptens and Conjugates. A schematic representation of the synthesis of three haptens is shown in Figure 2.

Hapten A, *4-(4-((2, 4-diaminopyrimidin-5-yl) methyl)-2, 6-dimethoxyphenoxy) butanoic acid (3)*, was synthesized as follows: Briefly, TMP (20 g, 68.9 mmol) was firstly added to the HBr (48%, 240 mL) in batches and then stirred at 100°C for 30 min. Then KOH solution (50%, 67 mL) was slowly added to the hot HBr solution to quench the reaction. Then, mixture was cooled to room temperature followed by stirring slowly to precipitate a white solid. The precipitate was filtered and then washed by ice water. The pH of the mixture was then neutralized to 7 using ammonia (28%) followed by filtering, washing and drying steps. The crude product was chromatographed and eluted with dichloromethane/methanol (20/1) to afford compound (1) (2.9 g, yellow powder). Cs_2CO_3 (6.84 g, 21 mmol) was added to a solution of compound (1) (2.9 g, 10.5 mmol) in DMF (35 mL) and stirred at room temperature for 20 min. Ethyl 4-bromobutyrate (3.29 g, 15.8 mmol) was added into the solution of compound (1) and the resulting mixture was stirred and refluxed at 40°C for 2 h. The mixture was extracted by ethyl acetate four times when it was cooled to room temperature. The obtained organic phases were combined, successively washed by water, saturated aqueous $NaHCO_3$ solution, saturated brine and then dried using anhydrous sodium sulfate. The crude product was chromatographed and eluted with the mixture of dichloromethane/methanol (25/1) to

afford compound (2) (3.2 g, yellow powder). Then, NaOH aqueous solution (2 mol L^{-1}, 24.6 mmol) was added to a methanol solution of compound (2) (3.2 g, 8.2 mmol in 35 mL) and stirred at 45°C for 2 h. After the mixture was cooled, methanol was rotary evaporated. The pH of the crude product which was dissolved in 8 mL water was neutralized to 7 using 1 mol L^{-1} HCl aqueous solution. The yellow precipitate which was obtained after stirring for 30 min was filtered and dried to obtain the final product of Hapten A (2.6 g, yellow powder). MS m/z 363.2. $[M-H]^-$; ^1H NMR (400 MHz, DMSO–d6): δ 7.50 (s, 1H), 6.54 (s, 2H), 6.19 (s, 2H), 5.86 (s, 2H), 3.80 (t, J = 6.0Hz, 2H), 3.70 (s, 6H), 3.52 (s, 2H), 2.41 (t, J = 7.2Hz, 2H), 1.75–1.82 (m, 2H).

Hapten B, *6-(4-((2, 4-diaminopyrimidin-5-yl) methyl)-2, 6-dimethoxyphenoxy) hexanoic acid (5)*. Hapten B was synthesized similar to the previous procedure. Compound (1) was reacted with ethyl 6-bromohexanoate to obtain Hapten B (2.5 g, yellow powder). MS m/z 391.2. $[M-H]^-$, ^1H NMR (400 MHz, DMSO-d6): δ 7.50 (s, 1H), 6.54 (s, 2H), 6.22 (s, 2H), 5.84 (s, 2H), 3.76 (t, J = 6.4Hz, 2H), 3.70 (s, 6H), 3.52 (s, 2H), 2.21 (t, J = 7.2Hz, 2H), 1.51-1.60 (m, 4H), 1.38-1.44 (m, 2H).

Hapten C, *4-((4-((2, 4-diaminopyrimidin-5-yl) methyl)-2, 6-dimethoxyphenoxy) methyl) benzoic acid (7)*. Hapten C was prepared with the similar procedure to that of Hapten A. Compound (1) was reacted with ethyl 6-bromohexanoate to obtain Hapten C (4.0 g, yellow powder). The MS m/z 411.1. $[M-H]^-$; ^1H NMR (400 MHz, DMSO-d6): δ 7.93 (d, J = 8.0 Hz, 2H), 7.56 (d, J = 8.0 Hz, 2H), 7.45–7.49 (m, 3H), 7.15 (s, 2H), 6.64 (s, 2H), 4.93 (s, 2H), 3.75 (s, 6H), 3.59 (s, 2H).

169 The three haptens with carboxylic acid groups were activated and coupled to a
170 protein (KLH, BSA or OVA) through the active-ester method. Firstly, 20 mg of each
171 hapten was dissolved in 0.6 mL DMF with the addition of NHS (10 mg) and DCC (20
172 mg). The mixture was reacted using a magnetic stirrer at 4°C for 5 h followed by the
173 removal of the precipitates. The supernatant of each hapten was divided into three
174 parts and then dropwise added into dissolved KLH solution (20 mg KLH in 9.5 mL
175 PBS), BSA solution (20 mg BSA in 9.5 mL PBS), and OVA solution (50 mg OVA in
176 10 mL PBS), respectively. The solutions containing the hapten-protein conjugates
177 were stirred for 12 h and then dialyzed in PBS for 2 days. Hapten-KLH served as an
178 immunogen and was stored at −70°C. Hapten-BSA and hapten-OVA acted as coating
179 antigens and then were stored at −20°C. The conjugation ratios of haptens-BSA were
180 characterized using MALDI–TOF-MS and were calculated as follows:

181 $$\text{Conjugation ratio} = \{M(\text{conjugates}) - M(\text{BSA})\}/M(\text{haptens}) \quad \text{(Eq.1)}.$$

182

183 **Production of Monoclonal Antibodies.** All animal treatments were in strict
184 accordance with Chinese laws and guidelines which were approved by the Animal
185 Ethics Committee of China Agricultural University. Fifteen eight-week old female
186 BALB/c mice were divided into three groups randomly (five mice per group) and
187 were immunized with three immunogens (Hapten A-KLH, Hapten B-KLH and
188 Hapten C-KLH). The mice were immunized three times with an interval of three
189 weeks between immunizations. First immunization, 100 μg prepared immunogen (1 g

L^{-1} in PBS) was mixed and emulsified with equal complete Freund's adjuvant. The prepared mixture was then injected into BALB/c mice (subcutaneously, 0.2 mL per mouse). For the second immunization, the mice were boosted with the mixture of immunogen (100 μg) and incomplete Freund's adjuvant. The procedure for the third immunization was the same as that for the second. Ten days after the third immunization, antisera samples (approximately 50 μL) obtained from the eye socket of mice were collected to detect the sensitivity and specificity based on the icELISA. The mice with a low IC_{50} and broad-specificity were selected for subsequent cell fusion. The cell fusion procedures were carried out as described previously.[28, 29] The selected mice were injected intraperitoneally with three times the immune dose (300 μg immunogen in 500 μL PBS buffer). Three days later, SP2/0 myeloma cells and splenocytes from the selected mice were mixed together for cell fusion under the assistance of PEG 1500. The successfully fusion cells were cultured in HAT medium for 7 days and the cell supernatant was screened using the icELISA. The homologous coating antigen (with a carrier protein of BSA) was used and the concentration was 0.35 mg L^{-1} for icELISA. The positive hybridoma with high sensitivity was then subcloned using the limiting dilution method. Subcloning was carried out three times and the optimum single cell mass was collected and cultured. Finally, one part of the hybridoma was cryopreserved, and another part was collected to produce ascites via intraperitoneal injection. The ascites collected from mice were extracted and purified by the saturated ammonium sulfate.[30] The isotypes of the purified mAbs were

211 characterized with the mice mAb isotyping kit.

212

213 **Development of ELISA.** The ELISA plates were firstly coated with coating
214 antigen (100 μL $well^{-1}$) which was diluted with CB buffer and then incubated at 4°C
215 for 12 h. The coating solution in the ELISA plates was then discarded. Blocking
216 buffer was then added to the plates (150 μL $well^{-1}$) which were placed in an incubator
217 for 2 h at 37°C. The standard solution (50 μL) of TMP (or other competitors) was
218 added to the wells as well as 50 μL of diluted mAbs solution. After an incubation of
219 30 min at 37°C, the plates were washed by PBST for two times. Goat anti-mouse IgG
220 (HRP labeled) (1:5000, 100 μL $well^{-1}$) was then added and incubated for 30 min at
221 incubator. 100 μL TMB substrate was added into wells and incubated for 15 min at
222 37°C after washing. Then 2 mol L^{-1} H_2SO_4 (50 μL $well^{-1}$) was used to stop the
223 enzymatic reaction and the OD values of 450 nm was measured.

224 The standard curves were fitted using the following equation:

225 $$Y = (A–B)/ [1+(X/C)^{D}] +B \quad \text{(Eq. 2)}$$

226 where A and B are the responses at high and low asymptotes of the curve,
227 respectively, C is the concentration of the targets resulting in 50% inhibition. D is the
228 slope at the inflection point of the sigmoid and X is the calibration concentration.

229 Nineteen compounds associated with the structure of TMP were diluted to
230 produce a series of concentrations to estimate the IC_{50} using the standard curves. The
231 CR was calculated using the subsequent formula:

232 $$CR = (IC_{50} \text{ of TMP}/IC_{50} \text{ of compounds}) \times 100\% \quad \text{(Eq. 3)}$$

233

234 **Optimization of ELISA.** To improve the performance of the ELISA, the
235 concentrations and pairing combinations of coating antigen and mAb, some
236 physicochemical parameters such as pH values, ionic strength and content of organic
237 solvent were optimized. The effects of these parameters were evaluated by the
238 A_{max}/IC_{50} ratio; A_{max} represents maximal absorbance, and IC_{50} was fitted using Eq. 2.

239

240 **Molecule Alignment and Electrostatic Potential Analysis.** All structures were
241 built in Gaussian 09 (Gaussian, Wallingford, CT, USA) according to the ASGs
242 configurations in the PubChem database. Then, DFT calculations with the B3LYP
243 functional and 6-311^{++} G (d, p) basis set were performed to optimize the molecules
244 using the Gaussian 09 package.[31-33] The fundamental vibrations were calculated by
245 the same method to confirm whether they were true minima or not. TMP was chosen
246 as the template molecule to align TBP. The Molecule Overlay dialog in Discovery
247 Studio 2016 (Accelrys Software, Inc., San Diego, CA, USA) was used to conduct
248 molecular alignment. The alignment root-mean-square value was introduced to
249 measure the degree of molecular superposition in each group. The Gaussian 09 and
250 Gaussian View 5 packages were employed to conduct the molecular electrostatic
251 potential (ESP) analysis. The minima and maxima of the ESP were used in the
252 Multiwfn software package and mapped onto the *Van der Waal* surface.

253

254 **Matrix Effect and Recovery.** ASGs negative chicken and milk were both
255 provided by the National Reference Laboratory for Veterinary Drug Residues
256 (Beijing, China). Five-gram chicken (in 50 mL tube) were put in an ultrasonic bath
257 for 5 min followed by the addition of 50% acetonitrile solution (5 mL for each tube).
258 Next, the mixture was agitated on a vortex mixer for 20 min and then centrifuged for
259 10 min at 3500 g. The supernatant was separated and then diluted with PBS to
260 evaluate the matrix effect using icELISA.[22] Milk samples were degreased by
261 centrifugation for 20 min at 8000 g. Defatted milk was diluted with PBS to eliminate
262 the matrix effect.[29]

263 Blank chicken and milk samples were spiked with TMP, DVD, OMP, BOP and
264 BQP at three different concentrations, respectively. After pretreatment, the samples
265 were diluted (20-fold for chicken samples and 15-fold for defatted milk) and
266 submitted to icELISA for recovery analysis. All the recovery data were detected in
267 triplicate (N = 3) using icELISA.

268

269 ■ RESULTS AND DISCUSSION

270 **Preparation of Haptens and Conjugates.** In previous reports, several strategies
271 for preparing TMP conjugates were proposed, resulting in antibodies which were
272 highly specific to TMP with moderate affinity (Table 1). Using those strategies, the
273 amino groups of TMP were direct derivatives of glutaric anhydride (GA) or maleic

anhydride, and then coupled to the carrier protein.[22-25] However, the amino groups on diaminopyrimidine are not typical and are difficult to react with other reagents. Moreover, the derivation of these two amino groups is not selective, and always results in mixed and unpurified conjugates. These studies did not obtain purified and identified haptens. The objective of the present study was to generate mAbs with broad-specificity for ASGs which can be used to establish a class-selective ELISA for determining the total range of ASGs. To produce antibodies which exhibit the desired broad specificity, the key is the structure of the haptens which should closely mimic the common part of target analytes, and maximize the steric, electronic and hydrophobic similarity to the parent molecules. In the case of ASGs, all analogs share the common structure of diaminopyrimidine (Figure 1a). Thus, it is highly possible to generate broad-specificity antibodies against all ASGs by introducing active groups on the trimethoxybenzene moiety. Of these ASGs, TMP is the most frequently used ASG and has been used as a start molecule to prepare generic haptens of ASGs. Previous research showed that haptens that possess spacer arms containing four to six carbons were acceptable and appropriately sustain epitopes to produce high quality antibodies.[34-36] Here, we synthesized three novel generic haptens by deriving butyric acid, caproic anhydride and benzoic acid on the *meta*-OCH_3 group of trimethoxybenzene, and introduced different spacer arms ending with a carboxyl group, which were named Hapten A, Hapten B and Hapten C, respectively (Figure 2). All haptens were purified and identified by mass spectrometry and nuclear magnetic

295 resonance spectroscopy (Figure S1 and Figure S2), and the results indicated that the
296 three haptens were successfully synthesized.

297 The haptens possessing active carboxyl groups were attached to the amino
298 groups of proteins using the active ester method; thus, the common moiety of ASG
299 was fully exposed to the immune system and could produce antibodies with
300 broad-specificity. The BSA conjugates were verified using MALDI–TOF–MS as
301 KLH and OVA were mixed with an indeterminate molecular weight, which could not
302 be accurately identified. An observable shift in the peak maximum of BSA conjugates
303 in comparison to the control protein was observed, proving that the haptens had been
304 successfully conjugated to the carrier protein (Figure S3). The calculated molar ratios
305 of the hapten: BSA were2.0:1 (Hapten A: BSA), 8.4:1 (Hapten B: BSA) and 18.9:1
306 (Hapten C: BSA), respectively. The haptens-KLH conjugates were then used as the
307 immunogen, while, haptens-BSA and haptens-OVA were used as the coating
308 antigens.

309

310 **Characterization of Antisera and mAb.** The antisera of three groups of mice
311 were monitored after the third immunization. Table S1 showed that all immunized
312 mice had a positive immune response with high titers (1/5000–1/30000). Five ASGs,
313 including TMP, DVD, OMP, BOP and BQP were used to determine the affinity
314 (expressed by IC_{50}) and specificity (expressed by CR) of antisera using the
315 homologous coating antigen. The results indicated that all antisera could recognize

316 ASGs with varied affinities (IC_{50} values of antisera were from 0.11 to 21.32 μg L^{-1}).
317 The mice, Hapten A-KLH-1# and Hapten A-KLH-3# exhibited relatively broad
318 specificity (CR > 42%) against ASGs. Furthermore, the antisera derived from Hapten
319 A-KLH-1# showed generally lower IC_{50} values than those of Hapten A-KLH-3#. In
320 mice immunized with Hapten B-KLH and Hapten C-KLH, the antisera showed a
321 lower CR towards OMP (CR < 36%) and BQP (CR < 19.7%) compared with those
322 for Hapten A-KLH. These results indicated that Hapten A seemed more effective in
323 producing antibodies with broad-specificity than Hapten B and Hapten C. A possible
324 reason for this is that caproic anhydride and benzoic acid in the spacer arm of Hapten
325 A and Hapten B both had large steric hindrance thus resulting in exposure of the
326 characteristic structure of TMP. Compared with other reports on the production of
327 TMP,[22-25] all antisera derived from the three immunogens provided lower IC_{50} values
328 ranging from 0.22–2.47 μg L^{-1} for TMP, indicating that the haptens prepared in the
329 present study had a more potent effect in inducing a strong immune response than the
330 immunogens previously reported. In addition to the more precise synthesis,
331 purification and identification of haptens and conjugates in this study, we conclude
332 that the high potency of these haptens may have been derived from the high polarity
333 of diaminopyrimidine which was distal to the protein and completely exposed to
334 immune system. The recognition of antibodies and haptens is mainly dependent upon
335 hydrogen bonding, electrostatic, and hydrophobic interactions.[37] The two amino
336 groups of diaminopyrimidine could have contributed to the high immune response

and then induced a high affinity antibody, while haptens reported by other groups exposed trimethoxybenzene with high hydrophobicity to the immune system, resulting in relatively lower affinity. However, this will be proved by separately immunizing diaminopyrimidine and trimethoxybenzene conjugates in our further research.

For the cell fusion experiments, the best mice were chosen i.e., Hapten A-KLH-1#, Hapten B-KLH-4# and Hapten C-KLH-3#. After screening and cloning three times, five hybridomas were obtained. In detail, mAb 5C4 and 9C9 were from Hapten A, 3B6 and 14G1 were from Hapten B, and 1F1 from Hapten C, respectively. The isotypes of all mAbs were determined and are shown in Table S2 and the preliminary characterization of mAbs are shown in Table S3. Although all mAbs showed highly affinity to TMP with IC_{50} values below 0.4 μg L^{-1}, only 5C4 showed broad-specificity towards other ASGs via homologous coating antigens.

Optimization and Development of icELISA. Aiming to improve the performance of icELISA, the concentration of mAbs and coating antigen, coating antigen types and several physicochemical factors related to the buffer were examined. As to competitive ELISAs, low concentrations of immunoreagents are required to obtain the best sensitivity.[38] Accordingly, the dilutions of immunoreagents were firstly optimized to get the lowest IC_{50} and the optimum A_{max} values in the range of 1.8–2.2 (A_{max} is the absorbance value without analyte). We use checkerboard assays to study

the effect of different dilutions for mAbs and coating antigen on the A_{max} of icELISA. The optimal dilutions of mAbs and coating antigens are summarized in Table S4, which shows that any mAbs could recognize any coating antigens and all dilutions of immunoreagents were above 1/20000. The highest dilutions of mAb and coating antigen were for mAb 3B6 and homologous coating antigen, Hapten B-OVA. It is well known that heterologous coating antigens usually lead to higher sensitivity and lower dilution of immunoreagents in a competitive ELISA. As the heterologous coating antigen could often result in a weak decrease in antibody recognition compared with the homogenous coating antigen, this allows the analyte to compete with the heterogeneous coating antigen at lower concentrations and higher sensitivity can be obtained.[39] Thus, the optimal pair of coating antigen types and mAbs were then tested using a two-point (0 and 0.4 μg L^{-1} TMP) competitive format and were evaluated by inhibition rate. The higher inhibition rate represents the higher sensitivity then better pair of coating antigens and mAbs. Figure 3a shows the inhibition rate of five mAbs and six coating antigens in the presence of 0.4 μg L^{-1} TMP. The affinities of mAbs (except 1F1) for TMP were improved using heterologous coating antigens. Interestingly, BSA coating antigens all produced higher inhibition rates than the OVA counterparts. Thus, Hapten C-BSA was selected for subsequent studies. The detailed parameters of the five mAbs paired with Hapten C-BSA in addition to the IC_{50} and CRs are listed in Table S1. The results demonstrated that the mAb 3B6 and 1F1 showed low CRs values for OMP (< 4.4%)

379 and BQP (< 3.2%), while, mAb 9C9 and 14G1 showed similar recognition profiles
380 with TMP (100%), DVD (> 49.6%), OMP (> 52.6%) and BOP (>893%), but not BQP
381 (CR < 24.6%). The mAb 5C4 recognized all ASGs (TMP, DVD, BOP, OMP and
382 BQP) with similar high affinity, and was used for further optimization and to develop
383 a class-selective icELISA for the qualitative detection of total ASGs.

384 Several physicochemical factors were further optimized including pH value (6.0,
385 6.5, 7.0, 7.4 and 8.0 for PBS), ionic strength (concentrations of NaCl were 0.05, 0.1,
386 0.2, 0.5 and 1.0 mol L^{-1}) and organic solvent (proportion of methanol and acetonitrile
387 were 0%, 1%, 5%, 10% and 20%). The A_{max}/IC_{50} ratio was chose to be the primary
388 criterion to evaluate the icELISA and the highest ratio value meant the highest
389 sensitivity. It can be seen that the ratio of A_{max}/IC_{50} was highest at pH 7.4 in the range
390 6.0 to 8.0 evaluated (Figure 3b). These results illustrated that slight pH differences in
391 the assay buffer obviously affected the icELISA performance. Similar to pH, the
392 influence of ionic strength on the icELISA showed a similar tendency. The ratio of
393 A_{max}/IC_{50} was better at an ionic strength of 0.1 mol L^{-1} (Figure 3c). Deviation from
394 this concentration was detrimental to the icELISA performance. In addition, organic
395 solvents are often chosen to extract ASGs from food matrices[35, 40]. Excessive organic
396 solvent can result in denaturation of antibodies and lower sensitivity of the icELISA.
397 Therefore, the assay must be tested to determine the tolerance of organic solvents.
398 Several buffers containing different concentrations of methanol or acetonitrile were
399 used for testing. As shown in Figure 3d and Figure 3e, a clear decrease in the

400 A_{max}/IC_{50} ratio was observed when the concentration of methanol was more than 10%
401 or the concentration of acetonitrile was more than 5%. The ELISA could be
402 performed with methanol concentrations up to 10% or acetonitrile concentrations up
403 to 5%. Thus, the optimum conditions (pH 7.4 and 0.1 mol L^{-1} NaCl in PBS buffer)
404 were used in subsequent experiments.
405
406 **Sensitivity and Specificity of the Optimized icELISA.** The sensitivity and
407 specificity of the icELISA was determined by conducting competitive assays for
408 ASGs and other analogs (structures shown in Figure 1b). The sensitivity of mAb 5C4
409 was evaluated using the icELISA calibration curve for ASGs, and showed that the
410 IC_{50} was 0.067 μg L^{-1}, 0.076 μg L^{-1}, 0.016 μg L^{-1}, 0.112 μg L^{-1} and 0.139 μg L^{-1} for
411 TMP, DVD, BOP, OMP and BQP, respectively (Figure 3f). The IC_{50} value of the
412 developed icELISA was 30 to 100-fold better than other reported immunoassays for
413 TMP. The limit of detection (LOD) of the icELISA we developed was 2.8 to 300-fold
414 lower than the LOD or visual limit of detection (vLOD) of reported immunoassays. [23,
415 24, 27]

416 The specificity of the icELISA was demonstrated by counting CRs against
417 nineteen compounds, including five ASGs, nine structurally related compounds and
418 five other antibiotics. It is not surprising that the icELISA showed no CRs (< 0.002%)
419 for other frequently used antibiotics such as sulfaguanidine, sulfamethizole,
420 sulfamerazine, norfloxacin and furazolidone. The IC_{50} values and CR of the icELISA

421 for ASGs and other structurally related compounds are summarized in Table S5. It can
422 be seen that mAb 5C4 only recognized the compounds that possessed both
423 diaminopyrimidine and metoxybenzene, which was supported by observing the
424 ignorable CR for 3,4,5-trimethoxycinnamic acid; gallic acid trimethyl ether;
425 3-(3,4,5-trimethoxyphenyl)propionic acid; 3,4,5-trimethoxyphenylacetic acid; 2,
426 4-diamino-6-(4-fluorophenyl)pyrimidine, pyrimethamine and 2, 4-diaminopyrimidine.
427 These compounds only contained one moiety of TMP, i.e., diaminopyrimidine or
428 metoxybenzene. It is reasonable that the mAb could not recognize the compounds
429 only containing metoxybenzene as this moiety was used to conjugate with protein and
430 then was blocked when exposed to the immune system. We thought that the mAb
431 could recognize DAP which was fully exposed to the immune system; however, the
432 unstable immune-complex of mAb-DAP may lead to a high dissociation rate constant
433 resulting in very low affinity.

434 It should also be noted that diaminopyrimidine and metoxybenzene must be
435 connected by methylene instead of carbonyl. For example, the structure of TBP is
436 extremely similar to TMP except for the connect group as mentioned above, and this
437 difference resulted in an almost 800-fold decrease in the IC_{50} value for TBP compared
438 to TMP (Table S5). The recognition profiles of mAb for TBP and TMP were not easy
439 to explain by only viewing the 2D-chemical structure; thus, we further examined the
440 possible recognition mechanism of mAb in terms of conformational and electronic
441 aspects. We aligned TMP with TBP based on their lowest conformations and expected

that these two molecules would not be well superimposed. As shown in Figure 4a, our expectation basically agreed with the alignment of these molecules. For concise purposes, only the backbone of hapten molecules are viewed without hydrogen atoms. The conformations of TMP and TBP were different to the orientation of metoxybenzene as we superimposed the common part of diaminopyrimidine. The dihedral angles between the pyrimidine ring and the benzene ring of TMP and TBP were 88.67° and 50.79°, respectively. The torsion angles of C_7-C_6-C_9-C_{11} were 118.6° for TMP and 16.3° for TBP. The introduction of carbonyl around the connection site of diaminopyrimidine (C_9) resulted in the benzene ring bending away with an approximately 100° difference in TBP compared with TMP, which may be partly responsible for the almost 800-fold decrease in mAb recognition ability. Complementary shape is an essential factor for molecules interacting with mAb, but not sufficient to complete the stable complex of hapten-antibody. The electronic contribution to antibody recognition was thought to be another important factor. As seen in Figure 4b, the exit of carbonyl on TBP induced an obvious change in atom partial charges in comparison with those of TMP, for example, the C2, C4 and C7 carbon (Figure 4b), which were maximally exposed to the immune system. To explain the difference in TMP and TBP in terms of conformation and electron distribution, the ESP displayed on *van der Waal* surfaces of global lowest energy conformation for TMP and TBP are shown in Figure 4c and 4d (in the same orientation as for Figure 4a). The ESP shows the potential energy of a proton placed at a point near the

463 molecule. The most positive potential energy is represented with blue areas which are
464 repulsive to a proton on the molecules. The most negative potential energy is
465 represented by red areas which are attractive to a proton. It is clear from Figure 4c
466 that the surface area in different ESP ranges of TMP and TBP represented similar but
467 obviously varied electrostatic potential characters. Furthermore, TBP has a stronger
468 area of negative potential (marked by arrow) which is associated with the carbonyl as
469 observed in Figure 4d. The comparisons in Figure 4 demonstrated that the connect
470 group between diaminopyrimidine and metoxybenzene markedly changed the whole
471 molecular conformations and electron distribution, and then resulted in low affinity.

472 The icELISA exhibited the highest CR with BOP (418.7%) and showed similar
473 CR with TMP (100.0%), DVD (88.2%), OMP (59.8%) and BQP (48.2%). Although
474 the other four ASGs are not commercially available, TXP, MTP, ADP and ICL, we
475 suggest that the mAb should recognize them with similar affinity to TMP. The
476 satisfactory CRs indicated mAb 5C4 was a group-specific antibody against the five
477 ASGs. The icELISA we developed had significant advantages in terms of sensitivity
478 and broad-specificity compared with the results of other authors.[22, 24-25]

479

480 **Matrix Effect and Recovery.** ASGs are widely used in the feeding of poultry
481 and dairy cows, thus chicken and milk samples were chosen to determine the matrix
482 effect and recovery. The matrix effect of samples can influence quantification of the
483 target. The clean-up step is frequently used to eliminate matrix effects. However,

direct dilution of samples is a simpler way of eliminating matrix effects in rapid screening methods, such as ELISA.[41, 42] Thus, in this study, the matrix effect of the extract was expected to be removed just by dilution due to the high sensitivity of the developed icELISA. Therefore, the pretreated chicken sample was diluted 10 times, 20 times and 40 times with PBS and the defatted milk was diluted 2-fold, 5-fold and 15-fold with PBS, respectively. The standard curves of TMP prepared in diluted samples were then compared with those in PBS to evaluate the matrix interferences (Figure 3g, 3h). The influence of the matrix on the performance of the icELISA decreased as the dilution factor increased. Despite a 40-fold dilution of chicken samples could farthest improve assay performance in term of A_{max}, the icELISA standard curve in 20-fold dilution of chicken samples was more consistent with that in PBS (Figure 3g). Accordingly, 20-fold dilution of chicken samples in PBS buffer was chosen to establish the calibration curves. The matrix effects of milk were avoided by 15-fold dilution using PBS buffer (Figure 3h). The calculated limits of detection (from IC_{10}) were observed at 0.06 μg kg^{-1}-0.8 μg kg^{-1} in chicken samples and 0.05 μg L^{-1}-0.6 μg L^{-1} in milk samples, which was below the MRL of ASGs. The linearity range (from IC_{20} to IC_{80}) is shown in Table 2.

The recovery and coefficient of variation (CV) of spiked samples were used to evaluate the effectiveness of sample preparation and utility of the icELISA. Negative samples were spiked with five individual ASGs (TMP, DVD, BOP, OMP and BQP) at three different concentrations to determine recoveries with the icELISA (Table 2).

505 The recoveries ranged from 75.2% to 94.6% with a CV lower than 13.2% in chicken
506 samples. The recoveries ranged from 75.3% to 101.4% and the CV between analyses
507 ranged from 5.7% to 14.3% in milk samples. These results demonstrated that the
508 icELISA based on mAb 5C4 was ultra-sensitive, class-selective and reliable for the
509 detection of ASGs in chicken and milk.
510

■ Support Information

Buffer used in this article; The structures and mass spectra, and ^{1}H NMR spectra of three haptens (Figure S1–S2), MALDI–TOF-MS result of hapten-BSA (Figure S3); Characterization of antiserum and mAbs (Table S1), the isotypes of mAbs (Table S2), preliminary characterization of all the mAbs (Table S3), optimum dilution of coating antigens and mAbs (Table S4), cross-reactivity of structurally related compounds with mAb 5C4 in the icELISA (Table S5).

518 ## ■ ACKNOWLEDGEMENTS

519 This work is supported by the Beijing Municipal Natural Science Foundation (No.

520 6182019) and China Agriculture Research System (CARS–36).

521

■ REFERENCES

(1) Yang, Y.; Liu, X.; Li, B.; Li, S.; Kong, X.; Qin, Z.; Li, J. Simultaneous determination of diaveridine, trimethoprim and ormetoprim in feed using high performance liquid chromatography tandem mass spectrometry. *Food Chem*. **2016**, *212*, 358–366.

(2) Wang, H.; Yuan, B.; Zeng, Z.; He, L.; Ding, H.; Guo, C.; Kong, X.; Wang, W.; Huang, X. Identification and elucidation of the structure of in vivo metabolites of diaveridine in chicken. *J. Chromatogr. B* **2014**, *965*, 91–99.

(3) Luo, H.; Zhang, L.; Xue, F.; Li, Y.; Wang, X.; Fei, C.; Zhang, C. Simultaneous determination of trimethoprim and diaveridine in tissues of chicken, porcine, and fish by hydrophilic interaction liquid chromatography–tandem mass spectrometry. *Food Anal. Method* **2014**, *7*, 308–317.

(4) Liu, Z.; Wu, Y.; Sun, Z.; Wan, L. Characterization of *in vitro* metabolites of trimethoprim and diaveridine in pig liver microsomes by liquid chromatography combined with hybrid ion trap/time–of–flight mass spectrometry. *Biomed. Chromatogr.* **2012**, *26*, 1101–1108.

(5) Wang, L.; Huang, L.; Pan, Y.; Kuča, K.; Klímová, B.; Wu, Q.; Xie, S.; Ahmad, I.; Chen, D.; Tao, Y.; Wan, D.; Liu, Z.; Yuan, Z. Metabolism and disposition of aditoprim in swine, broilers, carp and rats. *Sci. Rep*. **2016**, *6*, 20370.

(6) Huang, D. B.; Morrissey, I.; Murphy, T.; Hawser, S.; Wilcox, M. H. Efficacy evaluation of iclaprim in a neutropenic rat lung infection model with methicillin–

543 resistant *Staphylococcus aureus* entrapped in alginate microspheres. *Eur. J. Clin.*
544 *Microbiol. Infect. Dis.* **2018**, *37*, 673–678.
545 (7) White, G.; Daluge, S. M.; Sigel, C. W.; Ferone, R.; Wilson, H. R. Baquiloprim, a
546 new antifolate antibacterial: in vitro activity and pharmacokinetic properties in cattle.
547 *Res. Vet. Sci.* **1993**, *54*, 372–378.
548 (8) Song, N.; Zhang, S.; Li, Q.; Liu, C. Liquid chromatographic/mass spectrometry
549 assay of bromotetrandrine in rat plasma and its application to pharmacokinetic study.
550 *Biomed. Chromatogr.* **2009**, *23*, 623–629.
551 (9) Felix, J. P. F.; Lira, R. P. C.; Zacchia, R. S.; Toribio, J. M.; Nascimento, M. A.;
552 Arieta, C. E. L. Trimethoprim–sulfamethoxazole versus placebo to reduce the risk of
553 recurrences of *Toxoplasma Gondii* retinochoroiditis: randomized controlled clinical
554 trial. *Am. J. Ophthalmol.* **2014**, *157*, 762–766.
555 (10) Ono, T.; Sekiya, T.; Takahashi, Y.; Sasaki, Y. F.; Izumiyama, F.; Nishidate, E.;
556 Tsuda, S.; Ohta, T. The genotoxicity of diaveridine and trimethoprim. *Environ.*
557 *Toxicol. Pharmacol*. **1997**, *3*, 297–306.
558 (11) Ministry of Agriculture and Rural affairs in China. Regulation No. 235 of 24
559 December 2002 setting maximum residue levels of veterinary medical products in
560 foodstuffs of animal origin. *Regulation NO. 235,* **2002**.
561 (12) Commission Regulation (EC). No. 37/2010 of 22 December 2009 setting
562 maximum levels for certain contaminants in foodstuffs. *Off. J. Eur. Union* **2009**,
563 L15/67.

564 (13) Commission Regulation (EC). No. 37/2010 of 22 December 2009 setting
565 maximum levels for certain contaminants in foodstuffs. *Off. J. Eur. Union* **2009**,
566 L15/10.
567 (14) Department of Food Safety, Ministry of Health, Labour and Welfare. No.
568 0526004 of June 2006 for agricultural chemical residues in foods. *Japanese Positive*
569 *List System No. 0526004,* **2006**.
570 (15) Sichilongo, K. F.; Mutsimhu, C.; Obuseng, V. C. Gas chromatography–mass
571 spectral characteristics of six pharmacologically active compounds–analytical
572 performance characteristics on a raw sewage impacted water sample. *Can. J. Chem.*
573 **2013**, *91*, 704–710.
574 (16) Gavilan, R. E.; Nebot, C.; Patyra, E.; Miranda, J. M.; Franco, C. M.; Cepeda, A.
575 Simultaneous analysis of coccidiostats and sulphonamides in non–target feed by
576 HPLC–MS/MS and validation following the Commission Decision 2002/657/EC.
577 *Food Additives Contaminants: Part A* **2018**, 1–14.
578 (17) Cheng, L.; Zhang, S.; Shen, J.; Liu, J.; Lequn, W. Determination of trimethoprim
579 in feedstuffs by HPLC. *Journal of Instrumental Analysis* **2008**, *1*, 88–90.
580 (18) Isanga J.; Mukunzi D.; Chen Y. Development of a monoclonal antibody assay
581 and immunochromatographic test strip for the detection of amikacin residues in milk
582 and eggs. *Food Agr. Immunol*. **2017**, *28*, 668–684.
583 (19) Chen Y.; Liu L.; Xu L. Gold immunochromatographic sensor for the rapid
584 detection of twenty-six sulfonamides in foods. *Nano Res.* **2017**, *10*, 2833–2844.

585 (20) Isanga J.; Mukunzi D.; Chen Y. Development of a monoclonal antibody assay
586 and a lateral flow strip test for the detection of paromomycin residues in food
587 matrices. *Food Agr. Immunol*. **2017**, *28*, 355–373.
588 (21) Chen Y.; Guo L.; Liu L. Ultrasensitive immunochromatographic strip for fast
589 screening of 27 sulfonamides in honey and pork liver samples based on a monoclonal
590 antibody. *J. Agric. Food Chem*. **2017**, *65*, 8248–8255.
591 (22) Chen, Y.; Liu, L.; Song, S.; Kuang, H.; Xu, C. Establishment of a monoclonal
592 antibody–based indirect enzyme–linked immunosorbent assay for the detection of
593 trimethoprim residues in milk, honey, and fish samples. *Food Agric. Immunol.* **2016**,
594 *27*, 830–840.
595 (23) Chen, Y.; Liu, L.; Xie, Z.; Zhu, J.; Song, S.; Kuang, H. Gold
596 immunochromatographic assay for trimethoprim in milk and honey samples based on
597 a heterogeneous monoclonal antibody. *Food Agric. Immunol*. **2017**, *28*, 1–12.
598 (24) M Rtlbauer, E.; Meier, R.; Usleber, E.; Terplan, G. Enzyme immunoassays for
599 the detection of sulfamethazine, sulfadiazine, sulfamethoxypyridazine and
600 trimethoprim in milk. *Food Agric. Immunol*. **1992**, *4*, 219–228.
601 (25) Han, S.; Wu, X.; Jia, F.; Luo, X.; Wan, Y.; He, F. Preparation of monoclonal
602 antibodies to trimethoprim and ELISA kit for rapid detection. *Agriculture Science and*
603 *Technology* **2016**, *10*, 2267–2270.

(26) Wan, Y.; Feng, C.; Zhao, Z.; Zhang, Y.; Han, J. Study on gold immunochromatography assay for rapid detection of trimethoprim. *Dairy Industry* **2013**, *41*, 24–27.

(27) M Rtlbauer, E.; Usleber, E.; Schneider, E.; Dietrich, R. Immunochemical detection of antibiotics and sulfonamides. *Analyst* **1994**, *119*, 2543–2548.

(28) Zhang, X.; Eremin, S. A.; Wen, K.; Yu, X.; Li, C.; Ke, Y.; Jiang, H.; Shen, J.; Wang, Z. Fluorescence polarization immunoassay based on a new monoclonal antibody for the detection of the zearalenone class of mycotoxins in maize. *J. Agric. Food Chem.* **2017**, *65*, 2240–2247.

(29) Wang, Z.; Mi, T.; Beier, R. C.; Zhang, H.; Sheng, Y.; Shi, W.; Zhang, S.; Shen, J. Hapten synthesis, monoclonal antibody production and development of a competitive indirect enzyme–linked immunosorbent assay for erythromycin in milk. *Food Chem*. **2015**, *171*, 98–107.

(30) Zhang, X.; Wen, K.; Wang, Z.; Jiang, H.; Beier, R. C.; Shen, J. An ultra–sensitive monoclonal antibody–based fluorescent microsphere immunochromatographic test strip assay for detecting aflatoxin M1 in milk. *Food Control* **2016**, *60*, 588–595.

(31) Wang, Z.; Luo, P.; Cheng, L.; Zhang, S.; Shen, J. Hapten–antibody recognition studies in competitive immunoassay of α–zearalanol analogs by computational chemistry and pearson correlation analysis. *J. Mol. Recognit.* **2011**, *24*, 815–823.

624 (32) Zhang, F.; Liu, B.; Liu, G.; Zhang, Y.; Wang, J.; Wang, S. Substructure–activity
625 relationship studies on antibody recognition for phenylurea compounds using
626 competitive immunoassay and computational chemistry. *Sci. Rep.* **2018**, *8*, 3131.
627 (33) Arshad, M. N.; Asiri, A. M.; Alamry, K. A.; Mahmood, T.; Gilani, M. A.; Ayub,
628 K.; Birinji, A. S. Synthesis, crystal structure, spectroscopic and density functional
629 theory (DFT) study of
630 N-[3-anthracen-9-yl-1-(4-bromo-phenyl)-allylidene]-N-benzenesulfonohydrazine.
631 *Spectrochim Acta A* **2015**, *142*, 364–374.
632 (34) Wang, Z.; Beier, R. C.; Shen, J. Immunoassays for the detection of macrocyclic
633 lactones in food matrices–A review. *TrAC–Trend Anal Chem*. **2017**, *92*, 42–61.
634 (35) Vasylieva, N.; Barnych, B.; Rand, A.; Inceoglu, B.; Gee, S. J.; Hammock, B. D.
635 Sensitive immunoassay for detection and quantification of the neurotoxin,
636 tetramethylenedisulfotetramine. *Anal. Chem.* **2017**, *89*, 5612–5619.
637 (36) Lei, H.; Shen, Y.; Song, L.; Yang, J.; Chevallier, O. P.; Haughey, S. A.; Wang,
638 H.; Sun, Y.; Elliott, C. T. Hapten synthesis and antibody production for the
639 development of a melamine immunoassay. *Anal. Chim. Acta* **2010**, *665*, 84–90.
640 (37) Galve, R.; Camps, F.; Sanchez-Baeza, F.; Marco, M. P. Development of an
641 immunochemical technique for the analysis of trichlorophenols using theoretical
642 models. *Anal. Chem.* **2000**, *72*, 2237–2246.

643 (38) Abad, A.; Montoya, A. Development of an enzyme–linked immunosorbent assay
644 to carbaryl. 2. assay optimization and application to the analysis of water samples. *J.*
645 *Agric. Food Chem.* **1997**, *45*, 1495–1501.
646 (39) Wang, Z.; Liu, M.; Shi, W.; Li, C.; Zhang, S.; Shen, J. New haptens and
647 antibodies for ractopamine. *Food Chem.* **2015**, *183*, 111–114.
648 (40) Cliquet, P.; Cox, E.; Haasnoot, W.; Schacht, E.; Goddeeris, B. M. Generation of
649 group–specific antibodies against sulfonamides. *J. Agric. Food Chem.* **2003**, *51*,
650 5835–5842.
651 (41) Zhou, Q.; Peng, D.; Wang, Y.; Pan, Y.; Wan, D.; Zhang, X.; Yuan, Z. A novel
652 hapten and monoclonal–based enzyme–linked immunosorbent assay for sulfonamides
653 in edible animal tissues. *Food Chem*. **2014**, *154*, 52–62.
654 (42) Wang, Z.; Zhu, Y.; Ding, S.; He, F.; Beier, R. C.; Li, J.; Jiang, H.; Feng, C.; Wan,
655 Y.; Zhang, S.; Kai, Z.; Yang, X.; Shen, J. Development of a monoclonal antibody–
656 based broad–specificity ELISA for fluoroquinolone antibiotics in foods and molecular
657 modeling studies of cross–reactive compounds. *Anal. Chem.* **2007**, *79*, 4471–4483.

658 ■ **AUTHOR INFORMATION**

659 **Corresponding Author**

660 *E-mail: wangzhanhui@cau.edu.cn

661 **Notes**

662 The authors declare no competing financial interest.

663

664 # FIGURE CAPTIONS

665 **Figure 1.** The chemical structures used in the study: (a) Chemical structures of ASGs;
666 (b) Other compounds tested in the study.

667

668 **Figure 2.** The synthetic route of generic haptens.

669

670 **Figure 3.** The optimization of antigen-antibody pairs and physicochemcal parameters
671 on the icELISA and calibration curves assessed by the icELISA: (a) Inhibition rates of
672 different mAb-coating antigen pairs in the icELISA. The concentrations of mAbs and
673 coating antigens were optimized using checkerboard titration. The inhibition ratio was
674 calculated at the optimum concentration of mAbs and coating antigen when the OD
675 value ranged from 1.8 to 2.2. The effect of (b) pH value, (c) ionic strength, (d)
676 methanol and (e) acetonitrile on the icELISA (N = 3). Hapten C-BSA was used as
677 coating antigen and the concentration was 0.25 μg L^{-1}, TMP was used as a model
678 analyst for constructing the standard curves at 0.0033, 0.01, 0.03, 0.09, 0.27, 0.81 and
679 2.43 μg L^{-1}. Each value represents the average of three independent replicates. (f) The
680 icELISA standard curves based on mAb 5C4 for five ASGs in buffer. The icELISA
681 calibration curves for TMP in PBS and PBS diluted samples of (g) chicken, (h) milk.
682 Parallels were found between the standard curve prepared in PBS and diluted samples,
683 respectively (N = 3).

684

685 **Figure 4.** Molecular superposition and electrostatic potential energy of TMP and TBP.
686 (a) Superposition of the lowest energy conformation of TMP and TBP. Gray sections
687 represent carbon atoms, blue represent nitrogen atoms, red represent oxygen atoms
688 and light blue represent polar hydrogen atoms. (b) Calculated partial atomic charges
689 of selected atoms marked by the numbers shown in (a). (c) Surface area in each ESP
690 range on the *van der Waal* surface of TMP and TBP. (d) The structures optimized by
691 DFT and the ESP of TMB and TBP on the 0.001 a.u. contours of the electronic
692 density of the molecules. The negative ESP regions are indicated in red, and the
693 positive regions in blue.

Table1. Reported immunoassays for the determination of antibacterial synergists in the literature.

Haptens	Coupling method	Antibody type	IC_{50} ($\mu g\ L^{-1}$)	LOD/vLOD[a] ($\mu g\ L^{-1}$)	CR	Immunoassays	Related references
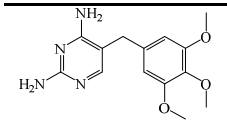	GA	pAb	6.0	6.0	TMP, 100%	ELISA	Erwin Martlbauer et al. (1992, 1994)
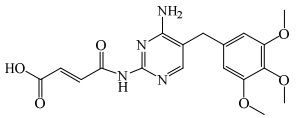	CDI[b]	mAb	–[c]	50	TMP, 100%	LFIA[d]	Yuping Wan et al. (2013)
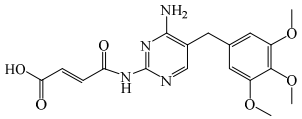	CDI	mAb	4.8	2.34	TMP, 100% DVD, < 1%	ELISA	Shen Han et al. (2016)
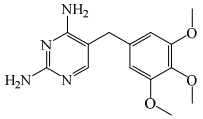	GA	mAb	4.14	–	TMP, 100% DVD, < 10%	ELISA	Yanni Chen et al. (2016)
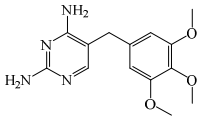	GA	mAb	1.98	10–15	TMP, 100% DVD, < 10%	LFIA	Yanni Chen et al. (2017)
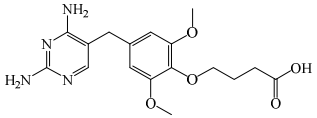	Active Ester	mAb	0.067	0.05–0.8	TMP, 100% DVD, 88.2% BOP, 418.7% OMP, 59.8% BQP, 48.2%	ELISA	This study

[a] vLOD refers to visual limit of detection of method.

[b] CDI refers to the carbodiimide method.

[c] Not exhibited in paper.
[d] LFIA is lateral flow assay.

Table 2. The LOD, linearity range, recovery and CV of five ASGs from spiked samples using the icELISA.

ASGs	Chicken					Milk				
	Spiked ($\mu g\ kg^{-1}$)	Recovery (%)	CV (%)	LOD[a] ($\mu g\ kg^{-1}$)	Linearity range[b] ($\mu g\ kg^{-1}$)	Spiked ($\mu g\ L^{-1}$)	Recovery (%)	CV (%)	LOD ($\mu g\ L^{-1}$)	Linearity range[b] ($\mu g\ L^{-1}$)
TMP	0.5	82.5	12.7	0.25	0.44−3.6	0.5	90.2	14.3	0.20	0.33−2.7
	1.5	89.6	10.4			1.5	87.8	5.7		
	3.5	94.3	8.5			2.5	101.4	8.0		
DVD	1.0	79.5	5.6	0.32	0.54−6.8	0.5	81.6	8.6	0.24	0.41−5.1
	3.0	83.3	8.3			2.0	90.5	12.2		
	6.0	94.6	12.1			5.0	87.1	9.8		
BOP	0.2	65.8	11.2	0.06	0.1−0.8	0.1	75.3	13.6	0.05	0.1−0.6
	0.5	69.1	10.6			0.3	78.4	10.9		
	0.8	75.9	9.6			0.6	89.6	12.9		
OMP	1.0	75.2	7.6	0.28	0.60−7.0	0.5	80.7	5.9	0.22	0.45−5.3
	3.0	80.9	5.2			2.0	92.6	11.7		
	6.0	87.6	11.5			5.0	91.9	7.6		
BQP	2.0	82.3	13.2	0.8	1.28−6.0	1.0	79.6	10.4	0.6	0.96−4.5
	4.0	92.3	10.6			2.0	95.8	12.4		
	6.0	87.6	9.6			4.0	89.7	12.1		

[a] The LOD was the concentration of standard showing a 10% inhibition (IC_{10}) in diluted chicken (20-fold) and milk (15-fold).

[b] The linearity range was calculated between IC_{20} and IC_{80} of the calibration curves in diluted chicken (20-fold) and milk (15-fold).

(a)

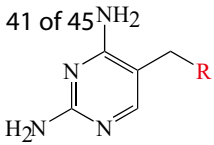

diaminopyrimidine
(common structure of ASGs)

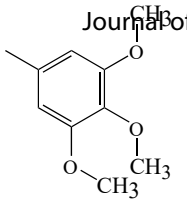

trimethoprim
（TMP）

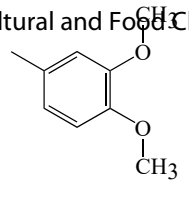

diaveridine
（DVD）

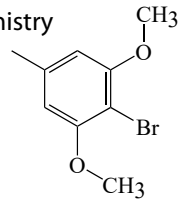

brodimoprim
（BOP）

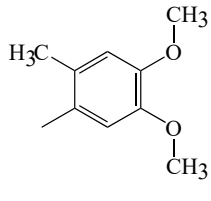

ormetoprim
（OMP）

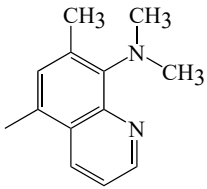

baquiloprim
（BQP）

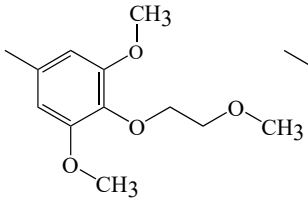

tetroxoprim
（TXP）

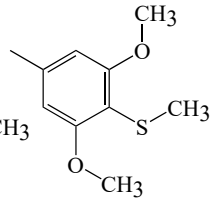

metioprim
（MTP）

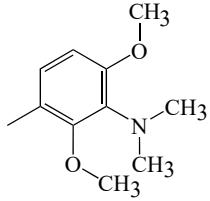

aditoprim
（ADP）

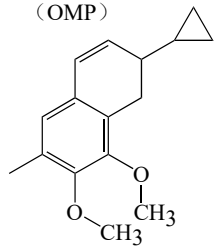

iclaprim
（ICL）

(b)

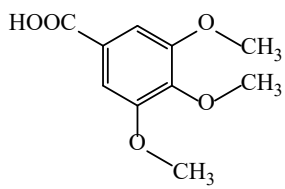

gallic acid trimethyl ether
(GATE)

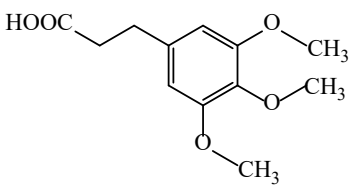

3-(3,4,5-trimethoxyphenyl)propionic acid
(TXR)

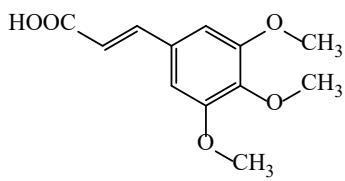

3,4,5-trimethoxycinnamic acid
(TXN)

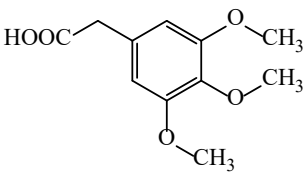

3,4,5-trimethoxyphenylacetic acid
(TXY)

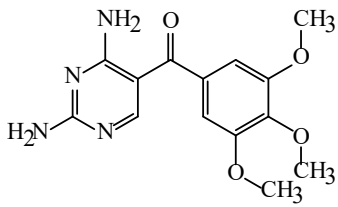

5-(3, 4, 5-Trimethoxybenzoyl)-2, 4-pyrimidinediamine
(TBP)

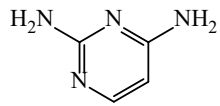

2, 4-diaminopyrimidine
(DAP)

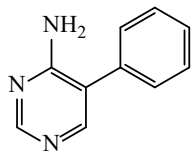

5-phenyl-4-pyrimidinamine
(PPY)

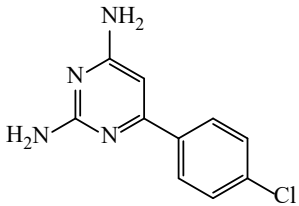

2, 4-diamino-6-(4-fluorophenyl)pyrimidine
(DFP)

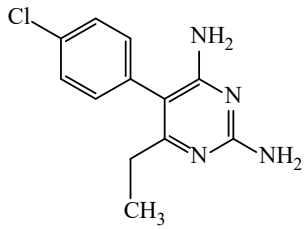

pyrimethamine
(PM)

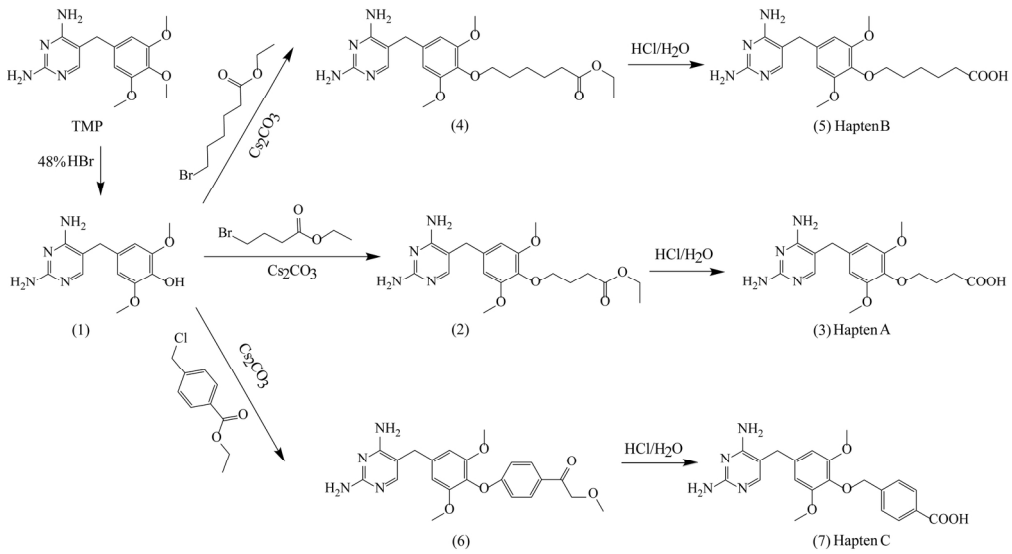

Figure 2

86x47mm (600 x 600 DPI)

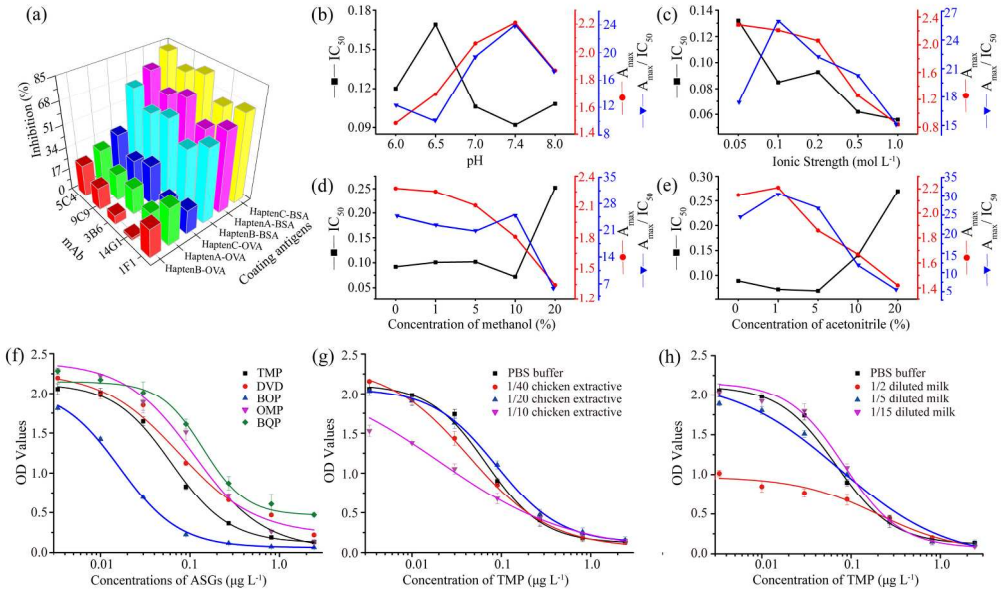

Figure 3

103x61mm (600 x 600 DPI)

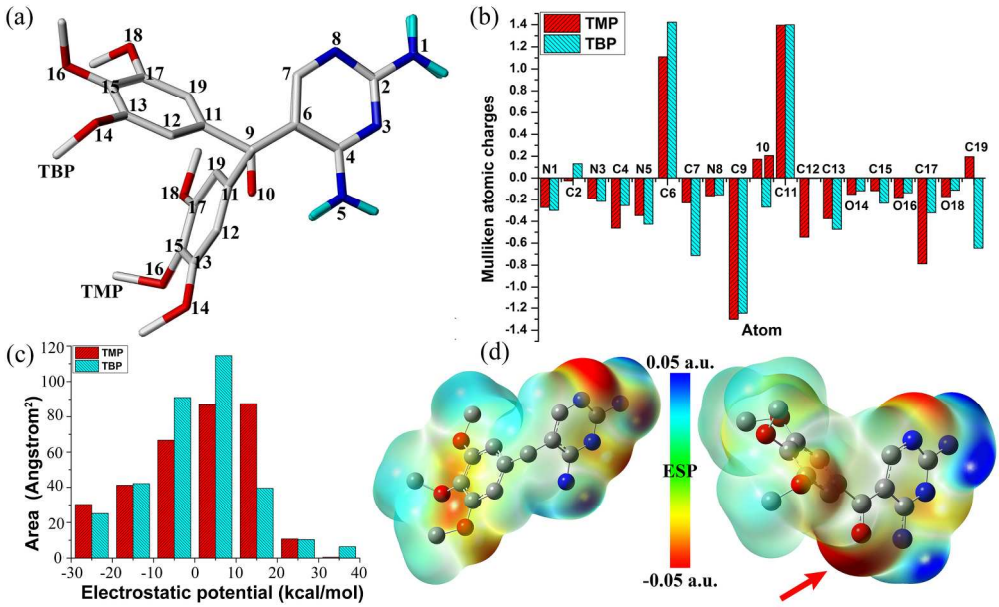

Figure 4

106x65mm (600 x 600 DPI)

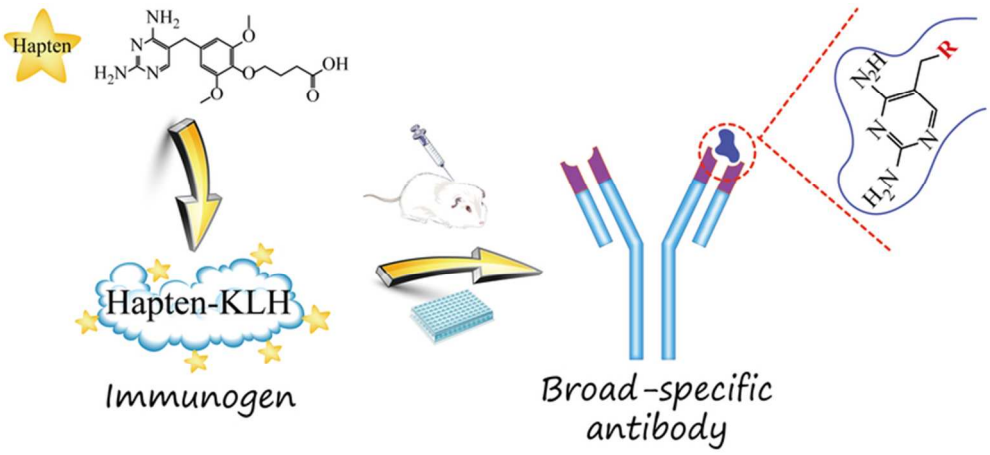

Table of content

34x15mm (600 x 600 DPI)